J Neurophysiol 126: 1090–1100, 2021.
First published August 18, 2021; doi:10.1152/jn.00303.2021

american physiological society

JNP JOURNAL OF NEUROPHYSIOLOGY

RESEARCH ARTICLE

Higher Neural Functions and Behavior

Hippocampal β2-GABA$_A$ receptors mediate LTP suppression by etomidate and contribute to long-lasting feedback but not feedforward inhibition of pyramidal neurons

Alexander G. Figueroa,[1]* Claudia Benkwitz,[1,2]* Gabe Surges,[1] Nicholas Kunz,[2] Gregg E. Homanics,[2] and Robert A. Pearce[1]

[1]*Department of Anesthesiology, University of Wisconsin-Madison, Madison, Wisconsin and* [2]*Department of Anesthesiology and Perioperative Medicine, University of Pittsburgh, Pittsburgh, Pennsylvania*

Abstract

The general anesthetic etomidate, which acts through γ-aminobutyric acid type A (GABA$_A$) receptors, impairs the formation of new memories under anesthesia. This study addresses the molecular and cellular mechanisms by which this occurs. Here, using a new line of genetically engineered mice carrying the GABA$_A$ receptor (GABA$_A$R) β2-N265M mutation, we tested the roles of receptors that incorporate GABA$_A$ receptor β2 versus β3 subunits to suppression of long-term potentiation (LTP), a cellular model of learning and memory. We found that brain slices from β2-N265M mice resisted etomidate suppression of LTP, indicating that the β2-GABA$_A$Rs are an essential target in this model. As these receptors are most heavily expressed by interneurons in the hippocampus, this finding supports a role for interneuron modulation in etomidate control of synaptic plasticity. Nevertheless, β2 subunits are also expressed by pyramidal neurons, so they might also contribute. Therefore, using a previously established line of β3-N265M mice, we also examined the contributions of β2- versus β3-GABA$_A$Rs to GABA$_{A,slow}$ dendritic inhibition, because dendritic inhibition is particularly well suited to controlling synaptic plasticity. We also examined their roles in long-lasting suppression of population activity through feedforward and feedback inhibition. We found that both β2- and β3-GABA$_A$Rs contribute to GABA$_{A,slow}$ inhibition and that both β2- and β3-GABA$_A$Rs contribute to feedback inhibition, whereas only β3-GABA$_A$Rs contribute to feedforward inhibition. We conclude that modulation of β2-GABA$_A$Rs is essential to etomidate suppression of LTP. Furthermore, to the extent that this occurs through GABA$_A$Rs on pyramidal neurons, it is through modulation of feedback inhibition.

NEW & NOTEWORTHY Etomidate exerts its anesthetic actions through GABA$_A$ receptors. However, the mechanism remains unknown. Here, using a hippocampal brain slice model, we show that β2-GABA$_A$Rs are essential to this effect. We also show that these receptors contribute to long-lasting dendritic inhibition in feedback but not feedforward inhibition of pyramidal neurons. These findings hold implications for understanding how anesthetics block memory formation and, more generally, how inhibitory circuits control learning and memory.

etomidate; GABA$_A$ receptors; general anesthesia; learning and memory

INTRODUCTION

Many drugs, including benzodiazepines, barbiturates, neurosteroids, and most general anesthetics, act as positive allosteric modulators of γ-aminobutyric acid type A receptors (GABA$_A$Rs) (1, 2). They produce a wide variety of effects, from anxiolysis, sedation, and memory impairment at low doses, to hypnosis, respiratory depression, and surgical immobility at higher doses. The spectrum of effects produced by a given drug is determined by both the dose that is administered and the subtype of GABA$_A$R that is targeted (3–5). Elucidating the mechanisms by which anesthetics produce their desired effects, and undesired side-effects, remains an important research goal.

* A. G. Figueroa and C. Benkwitz contributed equally to this work.
Correspondence: R. A. Pearce (rapearce@wisc.edu).
Submitted 2 July 2021 / Revised 2 August 2021 / Accepted 12 August 2021

GABA$_A$Rs are pentameric ligand-gated ion channels that collectively comprise the major class of inhibitory receptors in the mammalian brain (6). Each receptor is formed by five structurally similar transmembrane subunits that surround a central chloride-permeable ion pore. Each subunit exists in multiple isoforms (α1–6, β1–3, γ1–3, δ, ε, θ, and ρ1–3), with the majority of GABA$_A$Rs composed of two α, two β, and one γ subunit (7). Although there are millions of possible subunit combinations, it has been estimated that only ~25 different subunit combinations are present in the mammalian brain (8). The different receptor subtypes display distinct physiological properties and pharmacological sensitivities and their expression levels depend on brain region, developmental stage, cell type, and even subcellular location (9).

To link drug effects at the behavioral level to modulation of specific GABA$_A$R subtypes, one especially useful approach has been to study mice carrying mutations that make them insensitive to specific drugs. In particular, single point mutations in the transmembrane domains of β-subunits have been found that render those receptors insensitive to the general anesthetics etomidate and propofol (β2-N265S and β3-N265M) (10, 11) and partially insensitive to the inhaled agent isoflurane (12). Studies of mice carrying those mutations have been used to link specific β subunits to specific anesthetic endpoints—β3 to loss of righting reflex, respiratory depression, and loss of the hindlimb-withdrawal reflex (13, 14), and β2 to sedation and ataxia (15).

To test the contributions of β2- versus β3-GABA$_A$Rs to anesthetic-induced amnesia, we previously studied mice carrying the β3-N265M mutation (16). We found that they remained sensitive to the amnestic effect of etomidate and to suppression of long-term potentiation (LTP), a cellular model of learning and memory (17). This was an unexpected result because β3-GABA$_A$Rs are expressed at much higher levels than β2-GABA$_A$Rs in the hippocampus (18) and in a distribution pattern that matches that of α5 subunits (18, 19), which are essential targets for etomidate suppression of LTP and memory (20–22). There is also molecular evidence that α5 subunits preferentially associate with β3 subunits (23) and electrophysiological and pharmacological evidence that hippocampal pyramidal neurons predominantly express α5β3γ2 receptors (24, 25). However, as etomidate modulates only β2- or β3-GABA$_A$Rs (10), our experiments with β3-N265M mice thus showed that etomidate modulation of β2-GABA$_A$Rs alone is sufficient for its amnestic effect.

In the present study, we had two principal aims: *1*) to test whether the modulation of β2-GABA$_A$Rs is necessary for etomidate suppression of LTP, using a newly created line of mice carrying the β2-N265M mutation; and *2*) to test whether β2-GABA$_A$Rs contribute to long-lasting feedback or feedforward inhibition of pyramidal neurons, as recent reports have shown that long-lasting dendritic inhibition is particularly effective in controlling burst-induced NMDA-mediated depolarization, synaptic integration, and LTP (26, 27), and feedback and feedforward inhibition represent the canonical motifs by which inhibitory circuits control pyramidal cell excitation (28). We found that mice carrying the β2-N265M mutation were indeed resistant to LTP suppression by etomidate, confirming that modulation of β2-GABA$_A$R is essential for this anesthetic action. In whole cell recordings, we found that selective modulation of β2-GABA$_A$Rs slowed the decay of electrically evoked GABA$_{A,slow}$ inhibitory synapses, though to a substantially smaller degree than in wild-type (WT) mice. Using field potential recordings, we found that β2-GABA$_A$Rs are engaged in long-lasting feedback but not feedforward inhibition, whereas β3-GABA$_A$Rs are engaged in both. These results thus support an essential role for β2-GABA$_A$Rs in suppression of LTP by etomidate. They further demonstrate that β2-GABA$_A$Rs do contribute in part to long-lasting dendritic feedback inhibition, so modulation of this circuit might be instrumental in LTP suppression by etomidate. By the same token, we cannot exclude the possibility that etomidate exerts its amnestic effects through interneurons (16, 29), which in the hippocampus preferentially express β2-GABA$_A$Rs (18, 30, 31).

METHODS

All experiments were carried out with the approval of the Institutional Animal Care and Use Committees at the University of Wisconsin-Madison and the University of Pittsburgh.

Experimental Mice

β2(N265M) mice were generated on a C57BL/6J background using CRISPR-Cas9 technology with procedures described previously (32). Briefly, an in vitro transcribed gRNA with a target sequence (CCGGAGGTGGGTGTTGATTG) near the mutation site in Exon 9 of β2 was injected into C57BL/6J zygotes along with Cas9 mRNA and a 120-nucleotide single stranded oligonucleotide repair template (IDT DNA, Coralville, IA). A knockin founder was screened with PCR and Sanger sequencing for mutations at the top 15 off-target sites predicted in silico and identified mutations were eliminated from the pedigree following breeding with WT C57BL/6J mice. Experimental mice consisted of male and female homozygous WT and β2(N265M) littermates that were produced by heterozygous parents.

β3(N265M) mice were produced as previously described (14). Briefly, the β3(N265M) mutation was introduced by homologous recombination into a R1 (129/SvJ × 129/Sv) embryonic stem cell, and chimeric mice resulting from a single ES cell clone were bred in the 129/SvJ background. Four breeding pairs of mice heterozygous for the β3(N265M) mutation were obtained from University of Zurich (Dr. Uwe Rudolph). Experimental mice consisted of male and female homozygous WT and β3(N265M) littermates that were produced by heterozygous parents.

All mice were housed in the animal care facility under 12-h cycles of light and dark and had continuous access to standard mouse chow and water.

Genotyping

Tail samples were acquired from each mouse and genotyped either in-house using traditional, gel-based PCR methods, or sent to Transnetyx (Cordova, TN) which uses a TaqMan-based assay to collect real-time PCR data. For in-house PCR, primers were purchased from IDT (Integrated DNA Technologies, Coralville, IA). The primers used for in-house PCR were as follows: β2, 5′-AGGAAGGGTCACTAGGCAGA-3′ and 5′-TTGACATCCAGGCGCATCTT-3′; β3, 5′-GTTCAGCTTCCATTCTCACTG-3′ and 5′-GTTCAGCTTCCATT-

CTCACTG-3′. For the β2 line, the amplified DNA was digested using PagI. Samples sent to Transnetyx and genotyped using real time PCR amplification used the following primer sequences: β2, 5′-TTTTTTCAGGAATTACAACTGTC-CTAACAATG-3′ and 5′-GCACCCCATTAGGTACATGTCAAT-3′; β3, 5′-CCACCGTGCTCACCATGA-3′ and 5′-TCGATGGC-TTTGACATAGGGAATTT-3′.

Brain Slice Electrophysiology

Brain slice preparation: LTP studies.

Coronal hippocampal slices (400 μm) were prepared from 60–90 day old mice. Mice were deeply anesthetized using isoflurane and then decapitated. The brain was quickly extracted from the skull and immediately placed in ice-cold "cutting artificial cerebrospinal fluid" (cutting aCSF) saturated with carbogen (95% O_2/5% CO_2). The cerebellum was cut off at an ~15° caudo-rostral angle to produce an "off-coronal" cutting plane for slicing. The posterior end of the brain was glued to a metal stage and mounted onto the stage of a vibratome (Model 7000 smz2, Campden Instruments, Loughborough, UK) filled with ice-cold cutting aCSF. Brain slices were transferred into a submerged incubation chamber of elevated temperature (33°C) for 30 min, then for an additional 60 min at room temperature before being transferred into recording chambers for electrophysiology. Both recovery and recording solutions contained recording aCSF. Cutting aCSF consisted of (in mM): 124 NaCl, 3 KCl, 1.25 NaH_2PO_4, 25 $NaHCO_3$, 10 glucose, 1 sodium ascorbate, 3 kynurenic acid, 3.6 $MgSO_4$, and 0.8 $CaCl_2$. Recording aCSF consisted of (in mM): 124 NaCl, 3 KCl, 1.25 NaH_2PO_4, 25 $NaHCO_3$, 15 glucose, 0.8 sodium ascorbate, 1.3 $MgSO_4$, and 2.5 $CaCl_2$. All solutions were buffered to pH 7.3–7.4 when saturated with carbogen and had a recorded osmolality between 294–297 osmol/kgH_2O.

Brain slice preparation: whole cell IPSCs and feedback/feedforward inhibition.

Coronal hippocampal slices (400 μm) were prepared from 15–42 day [whole cell inhibitory postsynaptic currents (IPSCs)] or 30–180 day old mice (FB/FF inhibition). Mice were deeply anesthetized using 3% isoflurane and 70–100 mg/kg ketamine then decapitated. The brain was quickly extracted from the skull and immediately placed in ice-cold cutting aCSF saturated with carbogen (95% O_2/5% CO_2). The cerebellum was cut off at an ~15° caudo-rostral angle to produce an "off-coronal" cutting plane for slicing. The posterior end of the brain was glued to a metal stage and mounted onto the stage of a vibratome (Leica VT 1000S, Leica Microsystems Nussloch GmbH, Nussloch, Germany) filled with ice-cold cutting aCSF. Brain slices were transferred into a submerged incubation chamber at 35°C (IPSC recordings) or room temperature (FB/FF inhibition), where they remained for at least 60 min before being transferred into recording chambers for electrophysiology. Cutting aCSF consisted of (in mM): 127 NaCl, 1.88 KCl, 1.21 KH_2PO_4, 26 $NaHCO_3$, 10 glucose, 2.5 sodium ascorbate, 5 kynurenic acid, 1.44 $MgSO_4$, 11 $MgCl_2$, and 2.17 $CaCl_2$. Recording aCSF was identical to cutting aCSF, except that ascorbic acid, kynurenic acid and $MgCl_2$ were omitted. All solutions were buffered to pH 7.3–7.4 when saturated with carbogen and had a recorded osmolality between 290–300 mosmol/kgH_2O.

LTP studies.

Brain slices were place in a submersion-style recording chamber perfused with carbogen-saturated aCSF flowing at a rate of 3.0 mL/min. The temperature inside the chamber was maintained at 30°C using a TC-344C Automatic Temperature Controller (Warner Instruments, Hamden, CT). Slices were placed upon a custom-fabricated elevated mesh netting to allow for superfusion of both surfaces. For slice stability, platinum harps with thin nylon strings attached gently anchored the slices onto the netting. Recording pipettes (3–5 MΩ when filled with 1 M NaCl) were made of fire-polished borosilicate glass (OD 1.5 mm, ID 0.86 mm) pulled using a Model P-1000 micropipette puller (Sutter Instruments, Novato, CA). Tungsten bipolar electrodes were used for stimulation. Recording pipettes were inserted 80–120 μm into the CA1 *stratum radiatum* (SR) to measure field excitatory postsynaptic potentials (fEPSPs), and stimulating electrodes placed in SR ~1 mm from the recording electrode to evoke Schaffer collateral inputs to CA1 pyramidal cells. Input-output profiles were used to determine the stimulation intensity for the half-maximum fEPSP slope before baseline. All stimuli were biphasic and of 200-μs duration, at the intensity producing the 50% maximum fEPSP slope. Test stimuli were given at a rate of 0.05 Hz until a 30-min stable baseline was achieved. The θ burst stimulation (TBS) paradigm used to elicit LTP consisted of three trains of stimuli separated by 20 s, with each train consisting of 10 bursts of 4 pulses at 100 Hz, repeated every 200 ms. Recordings were continued for 60 min following TBS. To assure that etomidate was present at an equilibrium concentration, etomidate was added to the recovery solution as well as recording aCSF.

Stimulation and recording were controlled by WinLTP software (v2.3, Bristol University). Data were amplified ×1,000 and filtered between 0.1 Hz and 20 kHz using a Microelectrode AC Amplifier (Model 1800, A-M Systems, Everett, WA) and digitized at 40 kHz (National Instruments, Austin, TX). Stimulus timing outputs from WinLTP drove constant-current stimulus isolator units (WPI, Sarasota, FL; or STG 4004, MCS, Reutlingin, Germany).

Patch clamp recordings of IPSCs in CA1 hippocampal neurons.

Experiments were performed on the stage of an upright microscope (BX50WI, Olympus, Melville, NY) equipped with a long-working-distance water-immersion objective (Achroplan ×40; 0.75 numerical aperture; Carl Zeiss, Thornwood, NY) and differential interference contrast (Nomarski) optics. Brain slices were superfused at a rate of 2.8 mL/min with carbogen-saturated aCSF at room temperature (22°C–24°C). The microscope and recording pipette positions were controlled by an integrated motorized system (Luigs & Neumann, Ratingen, Germany). Recording pipettes were fabricated from borosilicate glass (1.7 mm OD, 1.1 mm ID; KG-33, Garner Glass, Claremont, CA) using a two-stage puller (Flaming-Brown model P-87, Sutter Instruments, Novato, CA). Pipettes were covered with Sylgard 184 (Dow Corning Company, Midland, MI) to reduce electrode capacitance and noise. Fire-polished open tip resistances were 2–4 MΩ when filled with recording solution consisting of (in mM): CsCl 140, Na-HEPES 10, EGTA 10, MgATP 2, QX-314 5, pH 7.3. Putative pyramidal cells in

stratum pyramidale (SP) of CA1 were visualized using a video camera (VE-1000; DAGE MTI, Michigan City, IN) equipped with an infrared bandpass filter (775 ± 75 nm). Access resistances were 10–20 mΩ and were then compensated 60%–80%. Cells were held at −60 mV. Evoked and spontaneous $GABA_A$ inhibitory postsynaptic currents (IPSCs) were pharmacologically isolated by bath application of 20 μM CNQX and 40 μM D-APV, to block AMPA/KA and NMDA receptor mediated currents and by the inclusion of CsCl and QX-314 in the patch pipette to block potassium currents and $GABA_B$ receptors. $GABA_{A,slow}$ currents were evoked by applying stimuli to the border of *stratum radiatum* (SR) and *stratum lacunosum-moleculare* (SLM) using a patch electrode filled with aCSF and a constant-current stimulus isolator (Model A365D, World Precision Instruments, Sarasota, FL). For SR/SLM stimuli, a maximum stimulation rate of 0.05 Hz was used to minimize the previously observed rundown of $GABA_{A,slow}$ over time (33). The position of the stimulating electrode and its stimulus intensity (50–300 μA) were adjusted until an isolated $GABA_{A,slow}$ event could be reliably elicited. All data were collected in voltage clamp mode using an Axopatch 200B patch clamp amplifier (Molecular Devices, San Jose, CA) and pClamp software (Molecular Devices). Data were filtered at 5 kHz, digitized at 10–20 kHz (Digidata 1200, Molecular Devices) and stored on computer hard disk for off-line analysis.

Extracellular recordings of feedback and feedforward inhibition.

Experiments were performed on the stage of an upright microscope (BX50WI, Olympus, Melville, NY) equipped with a ×10, 0.25 NA objective, using bright-field optics. Brain slices were superfused a rate of 2.8 mL/min with carbogen-saturated ACSF at room temperature (22°C–24°C). The same pipettes used for whole cell recording of IPSCs were used for field potential recordings. Open tip resistances were 2–4 MΩ when filled with recording aCSF. The recording electrode was placed in the SP layer of the CA1 region to record the population spike (PS) superimposed on the (passively sourced) fEPSP. Bipolar stimulating electrodes were fabricated from 100 kΩ tungsten recording electrodes (World Precision Instruments, Sarasota, FL). To study feedforward inhibition, we used a "Paired-Pulse Depression" (PPD) paradigm. A single stimulation electrode was placed in SR to evoke orthodromic population responses in CA1 neurons via activation of Schaffer collateral input. To study feedback inhibition we used a "Conditioned Depression" (CD) paradigm (34). In addition to the SR stimulating electrode, a second stimulating electrodes was placed in the *alveus* (ALV) to activate pyramidal cells antidromically, and thereby activate inhibitory interneurons targeted by pyramidal neurons (35, 36). Current pulses 0.1 ms in duration were delivered via constant current stimulus isolators (Model A365D, World Precision Instruments, Sarasota, FL) at a stimulus rate of 0.05 Hz. They were adjusted such that ALV stimulation (200–800 μA) elicited supramaximal and SR stimulation (60–250 μA) elicited half-maximal responses. Both PPD and CD responses were tested at interpulse intervals of 5-2000ms in the presence and absence of etomidate (1 μM).

All recordings were obtained in current clamp mode using an Axopatch 200B patch clamp amplifier (Molecular Devices) and pClamp software (Molecular Devices). Data were filtered at 5 kHz, digitized at 10–20 kHz (Digidata 1200, Molecular Devices) and stored on computer hard disk for off-line analysis.

Chemicals and Drugs

Unless stated otherwise, all chemicals were obtained from Sigma-RBI (St. Louis, MO). Ultrapure water was purified with a Millipore Milli-Q system (Billerica, MA) and used to prepare all solutions. Isoflurane was purchased from Abbott Laboratories (Abbott Park, IL) and Ketamine HCl from Lloyd Laboratories (Shenandoah, IA). Etomidate as a 0.2% (wt/vol) solution dissolved in propylene glycol (35% vol/vol) was obtained from Bedford Laboratories (Bedford, OH). This formulation was diluted 8,200-fold in aCSF to produce our experimental solutions for whole cell patch clamp and extracellular population spike recordings. We did not include propylene glycol in aCSF control solutions; we would note, however, that concentrations more than 100-fold greater were found in other hippocampal brain slice experiments not to influence population spikes (37). For LTP experiments, powdered etomidate was solubilized in DMSO to make a 50 mM stock solution. We did not include DMSO in our control aCSF solutions. We would note, however, that this solution was diluted 10^5-fold in aCSF, so that the DMSO concentration in our experimental etomidate-containing aCSF was tenfold lower than a 1:10,000 dilution, a commonly used standard for brain slice recordings, and 100-fold lower than 0.1% DMSO, which was found in other experiments not to influence LTP (38).

Data Analysis and Statistical Comparisons

Data were analyzed using WinLTP (v2.3, Bristol University), ClampFit 9.0 (Molecular Devices), Origin 9.0 (MicroCal, Northampton, MA), MS Excel (Microsoft, Redmond, WA), Prism 4.0 (GraphPad, San Diego, CA), and MATLAB (MathWorks Inc., Natick, MA). For LTP experiments, the maximum slope during the rising phase of the fEPSP was used as a measure of excitatory synaptic strength. The magnitude of LTP was defined as the average fEPSP slope during last 10 minutes of recording (i.e., 51–60 min after TBS) divided by the average slope of the 30 min preceding TBS. For whole cell recordings of IPSCs, evoked responses were fit to the exponential function $y = \Sigma\, A_n \exp[-t/\tau_n]$, where A_n and τ_n are the amplitude and the time constant of the *n*th component of a multiexponential fit. Goodness of fit was evaluated by visual inspection. To facilitate comparison of responses with differing numbers of decay constants we calculated and report here the weighted time constant $\tau_{wt} = \Sigma(A_n\tau_n)/\Sigma A_n$. For PPD, the amplitude of the PS elicited by the 2nd SR stimulus (conditioned) was divided by that elicited by the 1st (unconditioned). For CD, the amplitude of the PS elicited by the SR stimulus following ALV stimulus (conditioned) was divided by that elicited without a preceding ALV stimulus (unconditioned).

Results are expressed as means ± SE. Outliers were identified using an online InterQuartile Range test software package (https://www.statskingdom.com/outlier-calculator.html; $k = 1.5$) and excluded from further analysis. Comparisons of evoked IPSCs and PS amplitude for PPD and CD were carried out by one-tailed or two-tailed unpaired t-tests, as indicated,

or z-tests (unconditioned versus conditioned responses). P-values at or below 0.05 were deemed significant.

RESULTS

Etomidate Suppresses LTP through β2-GABA$_A$Rs

Our prior studies of β3-N265M mice, in which etomidate suppressed LTP in mutant as well as WT mice, implicated β2-GABA$_A$Rs in etomidate modulation of LTP (16). To test the role of β2-GABA$_A$Rs directly, we compared effects of etomidate on LTP of fEPSPSs in β2(N265M) versus WT mice (Fig. 1A). In the absence of etomidate, the magnitude of LTP was not different in slices from β2(N265M) versus WT mice (WT aCSF: 155 ± 8%; β2-N265M aCSF: 154 ± 5%; n = 8; P = 0.44). Etomidate (1 μM) strongly reduced LTP in brain slices from WT mice (WT etom: 118 ± 5%; n = 8; $P < 0.001$, one-tailed Student's t test), as expected based on prior studies (20, 29). However, etomidate failed to suppress LTP in brain slices from β2-N265M mice (β2-N265M etom: 148 ± 5%; n = 8; P = 0.213), confirming that β2-GABA$_A$Rs are an essential target of etomidate for LTP suppression.

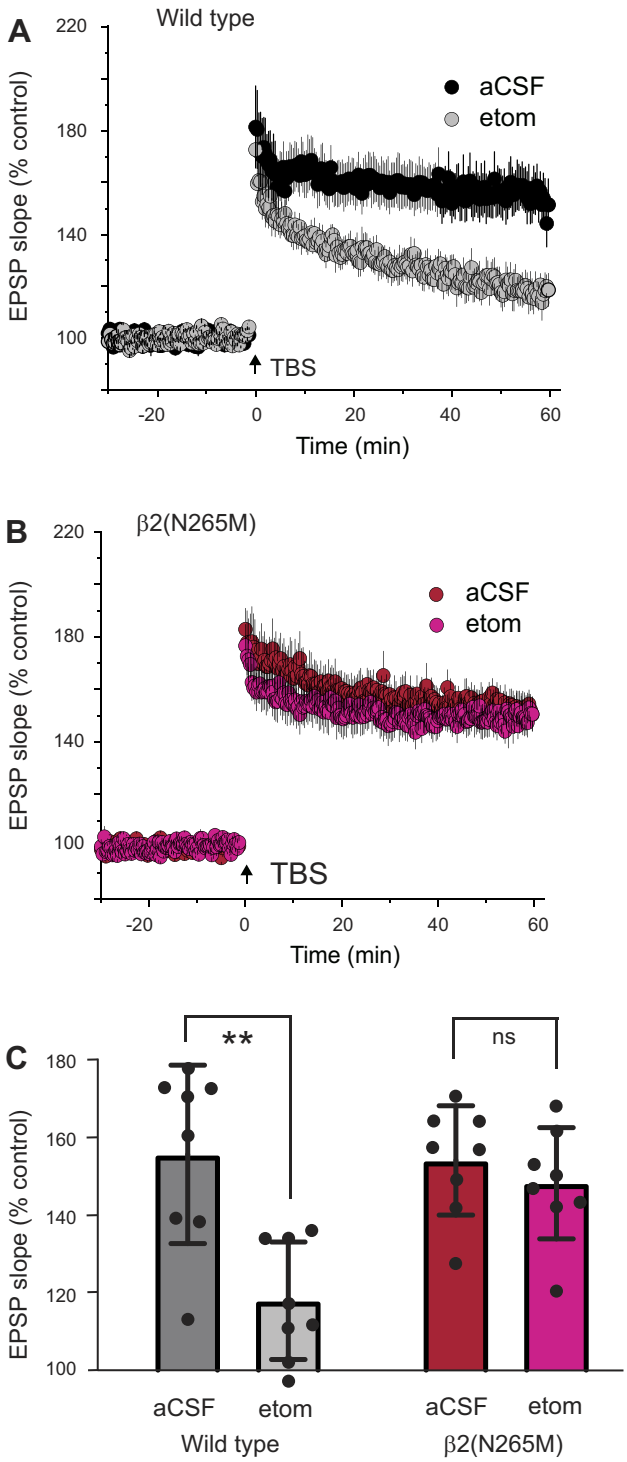

β2-GABA$_A$Rs Contribute to GABA$_{A,Slow}$ IPSCs

GABA$_A$R-mediated synaptic inhibition that targets CA1 pyramidal neuron dendrites is well suited to control NMDAR-mediated LTP, due to its spatial proximity to excitatory input, its slow kinetics matching NMDARs, and its nonlinear outward rectification (26, 27). These "GABA$_{A,slow}$" synapses are known to be mediated in part by α5 subunit-containing receptors in both neocortex and hippocampus (27, 39, 40), and they are reduced in β3-GABA$_A$R knockout mice. To determine whether β2-GABA$_A$Rs also contribute to GABA$_{A,slow}$ synaptic inhibition, we performed whole-cell patch clamp recordings of CA1 pyramidal neurons from WT mice and β3(N265M) mice (in which only β2-GABA$_A$Rs remain sensitive to etomidate), and elicited GABA$_{A,slow}$ currents using electrical stimuli. Experiments were performed in the presence of the glutamate receptor antagonists APV and CNQX. Results are shown in Fig. 2. In WT mice, etomidate prolonged the decay of evoked GABA$_{A,slow}$ IPSCs nearly 5-fold ($\tau_{wt,ctrl}$ = 78 ± 5 ms, $\tau_{wt,eto}$ = 370 ± 10 ms, n = 5). In β3(N265M) mice, etomidate also prolonged the decay of GABA$_{A,slow}$ IPSCs, but to a lesser degree than in WT mice ($\tau_{wt,ctrl}$ = 84 ± 10 ms, n = 5; $\tau_{wt,eto}$ = 205 ± 16 ms, n = 5; $P < 0.001$; $\tau_{wt,eto}$ versus $\tau_{mut,eto}$ P = 0.002, one-tailed t test). The decay of GABA$_{A,slow}$ IPSCs in aCSF did not differ between genotypes (P = 0.62, two-tailed t test). These results demonstrate that both β2- and β3-GABA$_A$Rs contribute to long-lasting dendritic inhibition in CA1 pyramidal neurons.

Roles of β2- and β3-GABA$_A$Rs in Feedforward and Feedback Inhibition

The results from whole cell patch clamp recordings presented above indicate that both β2- and β3-GABA$_A$Rs contribute to GABA$_{A,slow}$ dendritic inhibition. Are they activated by the same or different presynaptic sources? There are

Figure 1. Etomidate suppresses long term potentiation (LTP) through β2-GABA$_A$Rs. *A* and *B*: the extracellularly recorded field excitatory postsynaptic potential (EPSP) in the CA1 region in response to electrical stimulation of *stratum radiatum* was recorded in brain slices bathed in artificial cerebrospinal fluid (aCSF) alone or in the presence of etomidate (1 μM). After a 30-min stable baseline, LTP was induced by theta burst stimulation (TBS), in brain slices taken from wild-type mice (*A*) or mice carrying the β2 (N265M) mutation (*B*). The slope of the rising phase was normalized to the mean value for 30 min preceding TBS. Each point represents the means ± SE of 8 experiments. *C*: comparison of the average EPSP slope during the last 10 min of the recording, normalized to the 30-min baseline. Etomidate suppressed LTP in wild-type mice (**$P < 0.001$, one-tailed t test) but not β2(N265M) mice (P = 0.21, one-tailed t test).

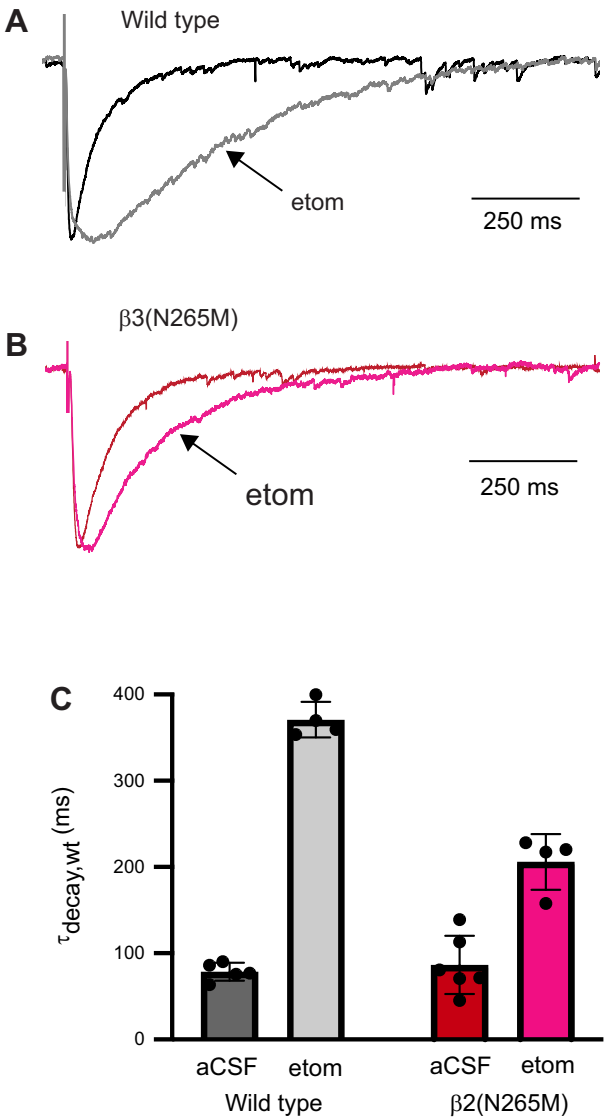

Figure 2. β2-GABA$_A$Rs contribute to GABA$_{A,slow}$ IPSCs in hippocampal pyramidal neurons. A and *B*: representative whole cell patch clamp recordings from CA1 pyramidal neurons, in response to electrical stimulation at the stratum radiatum/stratum lacunosum-moleculare border. Recordings were performed in the absence and presence of etomidate (etom; 1 μM). GABA$_A$R-mediated currents were isolated using QX-314 in the recording electrode to block GABA$_B$ receptors. The recording electrode was filled with a CsCl-based solution, so inhibitory currents are inward. Currents are normalized to the peak amplitude. *C*: average weighted decay time constants ($\tau_{decay,wt}$) for evoked GABA$_{A,slow}$ IPSCs recorded from wild type vs. β3(N265M) mice, in the absence and presence of etomidate. $n = 4$ or 5 for each genotype, error bars means ± SE. The decay rate did not differ between genotypes in the absence of etomidate ($P = 0.62$, two-tailed *t* test), but in the presence of etomidate it was significantly smaller in mutant mice compared to wild-type mice ($P = 0.002$, two-tailed *t* test). GABA$_A$Rs, γ-aminobutyric acid type A receptors; IPSCs; inhibitory postsynaptic currents.

several different classes of interneurons that target pyramidal neuron apical dendrites, and they can subserve either feedforward inhibition, or feedback inhibition, or both, depending on their excitatory drive. To determine whether β2- and β3-GABA$_A$Rs are differentially engaged by feedforward versus feedback inhibitory circuitry, we tested the effect of a preceding conditioning stimulus on the amplitude of the population spike (PS) evoked by SR stimulation, measuring the time-dependent suppression of the PS in brain slices from WT and β3(N265M) mice, in the absence and presence of etomidate.

To assess feedforward inhibition, the conditioning stimulus was the same as the SR test stimulus (Fig. 3*A*); we term this paradigm "paired-pulse depression" (PPD). In brain slices from WT mice under control conditions (aCSF only), the second stimulus of the pair produced a smaller response than the first only at the shortest interpulse intervals (Fig. 3, *B* and *D*). At longer IPIs, ranging from 20–300 ms, the second (conditioned) response was larger than the first (unconditioned) response, due to presynaptic facilitation of the afferent excitatory synapse. Etomidate caused the amplitude of the conditioned PS to be reduced at intervals ranging from 40–500 ms (aCSF versus etom, one-tailed *t* test; $n = 6$ for wild type, $n = 5$ for β3(N265M); $^*P < 0.05$, $^{**}P < 0.01$), consistent with its ability to enhance long-lasting dendritic inhibition (Fig. 2). In brain slices from β3(N265M) mice, responses were similar to those of WT mice under control conditions (Fig. 3, *C* and *D*), but etomidate failed to alter the conditioned response at any interpulse interval (aCSF versus etom, one-tailed *t* test; $n = 5$ for both genotypes; $P > 0.05$ at all IPIs). These results indicate that long-lasting feedforward inhibition is mediated entirely by β3-GABA$_A$Rs.

To assess feedback inhibition, the conditioning stimulus was applied to the alveus, where the CA1 pyramidal neuron axons are located (Fig. 4*A*); we term this paradigm "conditioned depression" (CD). In brain slices from WT mice under control conditions, the conditioned response (to stim 2 in the SR) was smaller than the unconditioned response (SR stim without prior stim 1) at all IPIs up to 300 ms (Fig. 4, *B* and *D*; *z*-test, $n = 5$, $P < 0.01$ at all intervals). Etomidate further depressed the conditioned response at all intervals ranging from 15–500 ms (paired *t* test, $n = 5$, $P < 0.05$ at all IPIs, $P < 0.01$ at IPI = 20–300 ms). In brain slices from β3(N265M) mice, the conditioned response in aCSF was reduced to a smaller extent compared to WT mice at intervals from 5–80 ms [one-tailed *t* test, WT vs. β3(N265M), $n = 5$ for each genotype, $P < 0.05$ at all IPIs, $P < 0.01$ at IPI = 5–40 ms]. Etomidate further depressed the conditioned PS, but only at intervals up to 150 ms (paired *t* test, $n = 5$, $P < 0.05$ at all IPIs). These results indicate that β2-GABA$_A$Rs do contribute to feedback inhibition at intervals up to 150 ms, and that β3-GABA$_A$Rs contribute over this same range, and also up to 500 ms. The difference in CD even in the absence of etomidate between WT and β3(N265M) mice indicates that the mutation itself reduces feedback inhibition, perhaps through changes in intrinsic receptor properties induced by the mutation (11). These results further support a partial contribution of β3-GABA$_A$Rs to feedback inhibition.

To summarize the contributions of β2- and β3-GABA$_A$Rs to feedforward and feedback inhibition, we plotted the fractional change in PS amplitude induced by etomidate in the two experimental paradigms (PPD and CD) for each genotype (Fig. 5). These graphs highlight the contribution of β2-GABA$_A$Rs to feedback inhibition at intervals up to 200 ms, and of β3-GABA$_A$Rs to both feedforward inhibition and feedback inhibition at intervals up to 500 ms.

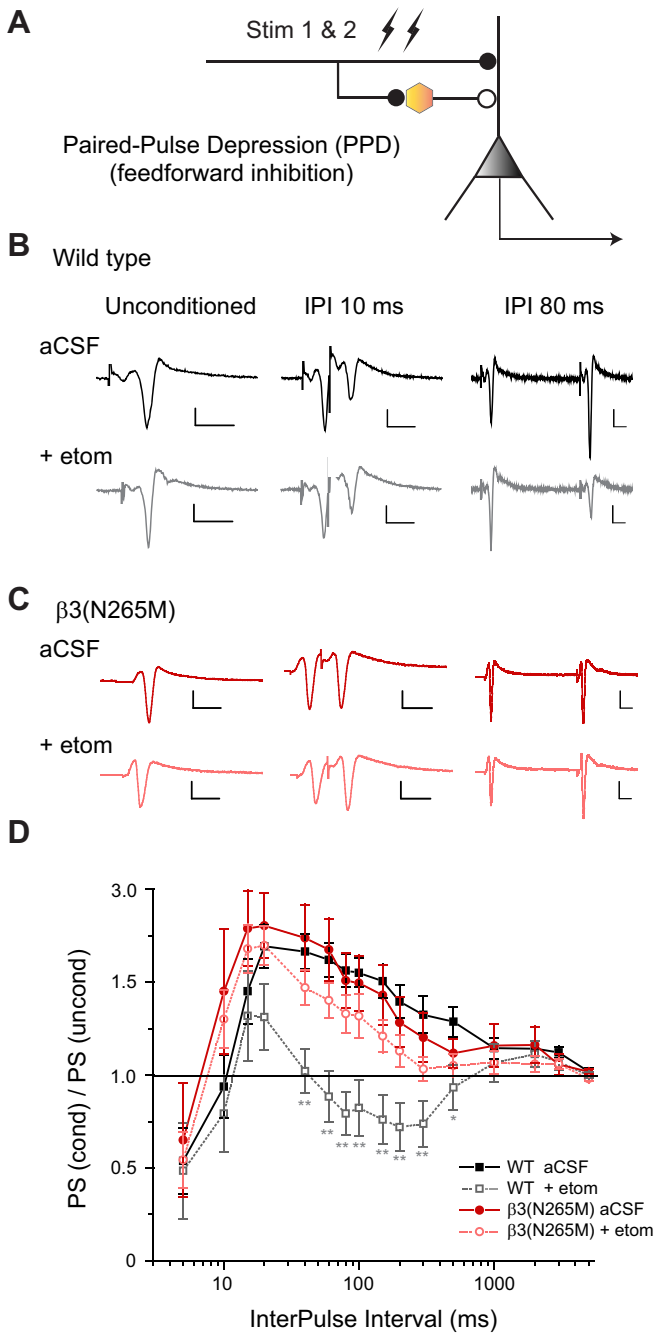

Figure 3. Effect of etomidate on feedforward inhibition. *A*: schematic diagram of the paired-pulse depression paradigm. Filled and open circles represent excitatory and inhibitory synaptic connections, respectively. *B*: extracellular field potentials in wild-type mice recorded from stratum pyramidale, in artificial cerebrospinal fluid (aCSF) alone or in the presence of etomidate (1 μM). The population spike (PS) in response to electrical stimulation of stratum radiatum is shown in the absence of a preceding stimulus (unconditioned) or for interpulse intervals (IPIs) of 10 and 80 ms. Note that in aCSF the response to the second pulse is reduced compare with the first at an IPI of 10 ms but greater at 80 ms, whereas in etomidate both are depressed. *C*: recordings similar to those shown in *B*, but in β3(N265M) mice. Note that etomidate does not alter the amplitude of the second PS at either IPI. *D*: the amplitude of the second (conditioned) spike divided by the first is plotted for IPIs ranging from 5 ms to 5 s. Each point represents the means ± SE of 5 (β3-N265M) or 6 (WT) experiments. $*P < 0.05$, $**P < 0.01$, aCSF vs. etom, one-tailed *t* test. Calibration bars: 10 ms, 0.5 mV.

DISCUSSION

The primary findings from this study are: *1*) etomidate modulation of β2-GABA$_A$Rs is essential to its ability to

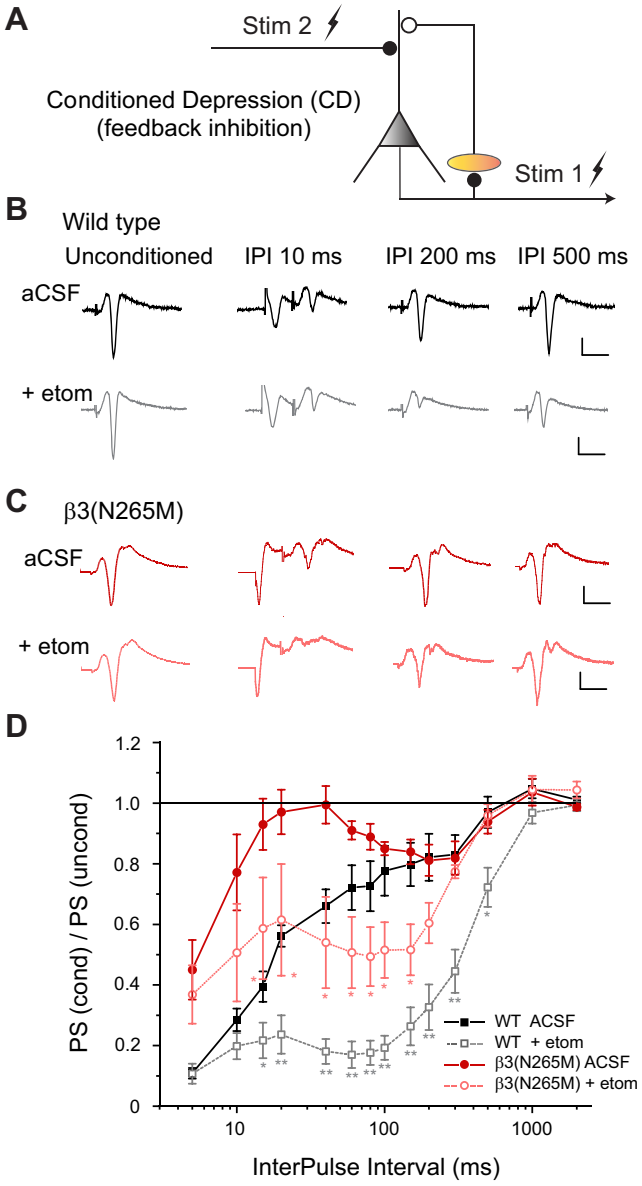

Figure 4. Effect of etomidate on feedback inhibition. *A*: schematic diagram of the conditioned depression paradigm. Filled and open circles represent excitatory and inhibitory synaptic connections respectively. *B*: extracellular field potentials in wild type mice recorded from stratum pyramidale, in artificial cerebrospinal fluid (aCSF) alone or in the presence of etomidate (1 μM). The population spike (PS) in response to electrical stimulation of stratum radiatum (SR) is shown in the absence of a preceding stimulus (unconditioned) or when preceded by a conditioning stimulus to the alveus, at interpulse (IPI) intervals of 10, 200, and 500 ms. Note that in aCSF, the response to the SR stimulus pulse is reduced at IPIs of 10 and 200 ms but not at 500 ms, whereas in etomidate all are depressed. *C*: recordings similar to those shown in *B*, but in β3(N265M) mice. Note that etomidate does not produce as large an effect at the longer IPIs. *D*: the amplitude of the conditioned PS divided by the unconditioned PS is plotted for IPIs ranging from 5 ms to 2 s. Each point represents the means ± SE of 5 experiments. $*P < 0.05$, $**P < 0.01$, aCSF vs. etom, one-tailed *t* test. Calibration bars: 10 ms, 0.5 mV.

suppress LTP in hippocampal CA1 neurons; *2*) both β2- and β3-GABA$_A$Rs contribute to dendritic GABA$_{A,slow}$ inhibitory currents; and *3*) β2-GABA$_A$Rs contribute to an early component of feedback inhibition, but not to feedforward inhibition in the CA1 region of the hippocampus, whereas β3-GABA$_A$Rs contribute to both. These findings indicate that if etomidate acts by modulating pyramidal neuron β2-GABA$_A$Rs, it is through the early component of feedback inhibition.

LTP Suppression by Etomidate

The mechanism by which a wide variety of drugs produce the constellation of behavioral changes that constitute "general anesthesia" remains undefined but of considerable interest. In recent years, it has become clear that each "end point," such as hypnosis, immobility, and amnesia, is brought about by anesthetic modulation of distinct brain regions, cellular elements, and molecular targets. To deduce the mechanisms for specific end points, etomidate has been studied heavily, because (at concentrations that are obtained clinically) it acts on a quite restricted range of targets: GABA$_A$Rs that incorporate either β2 or β3 subunits (10). However, even within this restricted range, etomidate's ability to bring about several end points have been traced to modulation of distinct subsets of receptors. Our recent report that β3-N265M mice remain sensitive to etomidate suppression of LTP and contextual fear conditioning implicated β2-GABA$_A$Rs (16). Our present findings confirm that β2-GABA$_A$Rs are essential to LTP suppression by etomidate.

Dendritic Inhibition of Pyramidal Neurons

How might enhancement of synaptic inhibition suppress LTP? One possibility is through GABA$_A$Rs on pyramidal neurons. Three physiologically distinct types of inhibition are found in pyramidal neurons: *1*) rapidly decaying synaptic currents (GABA$_{A,fast}$) that are produced by perisomatic targeting interneurons such as basket cells and axoaxonic cells; *2*) slowly decaying synaptic currents (GABA$_{A,slow}$) that are produced by dendrite-targeting interneurons including somatostatin-expressing O-LM cells and neurogliaform cells (NGFCs) activating α5-GABA$_A$Rs (27); and *3*) a tonic background current that is mediated by α5-GABA$_A$Rs (41). Enhancement of tonic inhibition has been proposed to underly suppression of LTP and memory (21), but GABA$_{A,slow}$ inhibition also has several characteristics that make it particularly well suited to controlling synaptic plasticity. These include *1*) its location proximate to excitatory synapses, *2*) its prolonged duration matching NMDAR-mediated currents, and *3*) its pronounced rectification, which enhances its ability to counteract voltage-dependent amplification of dendritic depolarizing signals (26, 27).

Our prior studies using a β3-subunit knockout mouse had implicated β3-GABA$_A$Rs in GABA$_{A,slow}$ synaptic inhibition (42). Our present findings confirm that result, demonstrating that β3-GABA$_A$Rs mediate a major portion of the GABA$_{A,slow}$ IPSC evoked by dendritic layer stimulation, and that they are solely responsible for feedforward inhibition, as well as the late component of feedback inhibition that extends beyond 200 ms under the influence of etomidate. From the present results, we are not able to determine which α-subunits partner with β3-subunits, but several lines of evidence point to α5-subunits: *1*) α5-subunits contribute to GABA$_{A,slow}$ IPSCs (40, 43); *2*) electrophysiological and pharmacological characteristics of acutely dissociated hippocampal pyramidal neurons indicate that the α5β3γ2 subunit combination constitutes the majority of receptors (24); *3*) the distribution pattern of β3 subunits in the hippocampus that matches that of α5 subunits (18, 19); and *4*) α5 subunits preferentially associate with β3 subunits (23). This same subunit combination (α5β3γ2) is also the likely source of tonic inhibition, as tonic inhibition in CA1 pyramidal neurons is mediated by α5-GABA$_A$Rs (41), and it is insensitive to etomidate in β3-N265M mice, indicating that it is produced entirely by β3-GABA$_A$Rs. Taken together, these findings indicate that tonic inhibition and GABA$_{A,slow}$ are likely produced by a single population of α5β3γ2 receptors that can move between extrasynaptic and synaptic sites under the regulation of phosphorylation and anchorage by radixin to the cytoskeleton (44). Our prior studies showing that β3-N265M mice remain sensitive to LTP suppression by etomidate (16), and our present studies showing that β2-N265M mice are resistant, indicate that neither tonic inhibition nor the β3-GABA$_A$R component of GABA$_{A,slow}$ inhibition are essential to LTP suppression by etomidate.

As β2-GABA$_A$Rs mediate a portion of feedback-activated GABA$_{A,slow}$ inhibition, could they underlie LTP suppression by etomidate? β2- and β3-GABA$_A$Rs are apparently not intermingled at GABA$_{A,slow}$ synapses, as feedforward inhibition exclusively activates β3-GABA$_A$Rs, whereas feedback inhibition activates both (Figs. 4 and 5). It is

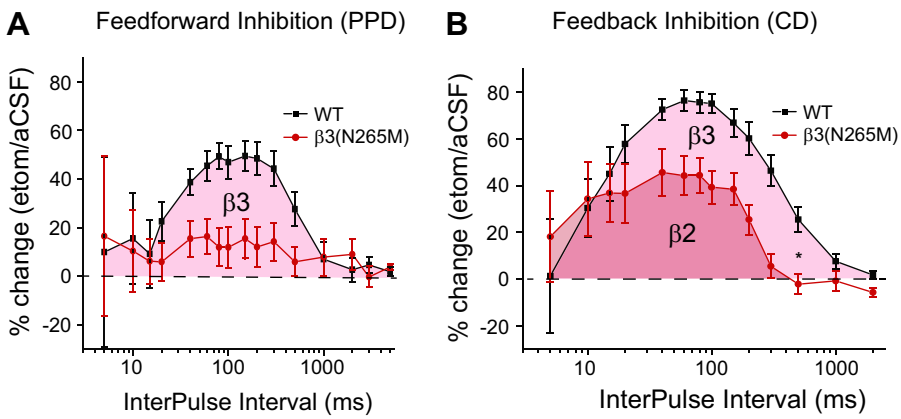

Figure 5. Summary of etomidate modulation of feedforward and feedback inhibition. The fractional change (expressed as a percentage) in the conditioned response, in the presence of etomidate, divided by that in aCSF, is plotted for interpulse intervals ranging from 5 ms to 5 s, for wild-type (WT) and β3(N265M) mice. *A*: the effect of etomidate in WT mice was absent in β3(N265M) mice at all intervals, indicating that β3-GABA$_A$Rs account entirely for feedforward inhibition. *B*: the effect of etomidate was partially reduced at intervals up to 200 ms, and entirely absent at longer intervals, indicating that β2-GABA$_A$Rs contribute to the early component of feedback inhibition, whereas β3-GABA$_A$Rs to both early and late components.

possible that feedback inhibitory pathways that utilize β2- versus β3-GABA$_A$Rs contact different locations within the dendritic tree, whether segregated along the proximo-distal axis, or on different branches, and that these different dendritic inhibitory influences are differentially effective in controlling the depolarization needed to initiate synaptic plasticity. Another possibility is that presynaptic sites that innervate β2- versus β3-GABA$_A$Rs differ in their use-dependent characteristics, and synapses that exhibit use-dependent depression versus facilitation might differentially influence LTP. Although we know of no direct evidence to support either of these possibilities, it is known that excitatory signaling and dendritic spikes can be confined to individual branches (45), and that both facilitating and depressing inhibitory synapses occur (46, 47). Therefore, it is possible that etomidate suppresses LTP by modulating a distinct subset of slow inhibitory synapses on pyramidal neurons that utilize β2-GABA$_A$Rs.

From the present experiments we cannot determine which α subunits co-assemble with β2 subunits in this component of GABA$_{A,slow}$. However, since β2-subunits preferentially assemble with α1 subunits (48), and only a portion of GABA$_{A,slow}$ is mediated by α5-subunits (40, 43), receptors composed of α1β2γ2 are one possibility. β2-GABA$_A$Rs can also coassemble with α5 subunits, and these receptors display deactivation characteristics that are faster than α5β3γ2 receptors (49), consistent with the weaker prolongation of GABA$_{A,slow}$ that we observed in our whole-cell recordings (Fig. 2). Therefore, α5β2γ2 receptors may also underlie a portion of feedback dendritic inhibition.

Which cells might be involved in long-lasting feedforward and feedback inhibition? Somatostatin-expressing oriens-lacunosum-moleculare (O-LM) interneurons receive excitatory input from pyramidal neurons, and they produce a synaptic current in pyramidal neurons that has a decay rate that is intermediate to somatic GABA$_{A,fast}$ currents from basket cells versus dendritic GABA$_{A,slow}$ currents from neurogliaform cells (35, 50). Therefore, O-LM interneurons likely contribute to the early component of β2-GABA$_A$R mediated feedback inhibition (Fig. 5). Ivy cells, which share developmental origins and some properties with neurogliaform cells (51–53), including a very dense axonal arbor that supports slow IPSC generation by volume transmission, target pyramidal neuron basal and oblique apical dendrites with a long-lasting feedback inhibition (54), so they are likely candidates for the late β3-mediated component of feedback inhibition. Since their dendritic arbor extends throughout stratum oriens and stratum radiatum (54), they might also receive excitatory input from CA3 pyramidal neurons and thus also mediate long-lasting feedforward inhibition, but this possibility remains speculative. Like ivy cells, neurogliaform cells generate large and long-lasting IPSCs (55), and they are known to be activated in a feedforward fashion, but primarily by perforant path inputs (56).

Slow α5β2-Mediated Inhibition of Interneurons

Rather than acting through pyramidal neurons, it is possible that etomidate instead, or in addition, suppresses LTP (and by extension memory) by modulating β2-GABA$_A$Rs on interneurons. Indeed, in the hippocampus, immunohistochemical (18, 31), and transcriptomic analysis (57) indicate that β2-GABA$_A$Rs are found primarily on interneurons. Importantly, α5 subunits are also found on interneurons (30, 58), though at lower levels than on pyramidal neurons (59). Etomidate action through interneurons that express α5β2-GABA$_A$Rs would be consistent with our previous finding that eliminating α5 subunits selectively from pyramidal neurons did not render brain slices insensitive to LTP suppression, though global α5-knockout did (29).

If etomidate does suppress LTP by enhancing β2-mediated inhibition of interneurons, which classes of interneurons might be involved? Useful clues might come from an examination of α5 subunit distribution. The clearest physiological evidence for α5-GABA$_A$R-mediated IPSCs in interneurons comes from studies of O-LM interneurons, where α5 subunits contribute to slowly decaying IPSCs made by vasoactive intestinal peptide (VIP)- and calretinin-positive interneurons onto the dendrites (58, 60). Enhancement of this inhibitory influence would then suppress O-LM firing, interrupting a disinhibitory input onto SR interneurons that supports LTP (61). In addition, slow IPSCs made by neurogliaform cells onto other neurogliaform cells, as well as autaptic synapses, are mediated in part by α5 subunits (50). By virtue of their developmental, anatomic, and physiological similarities with neurogliaform cells (51–53), ivy cells might also receive α5-mediated inhibitory inputs, but again this remains speculative.

It is interesting that both O-LM and neurogliaform/ivy interneurons target the dendrites of pyramidal neurons. For neurogliaform cells at least this occurs through α5-GABA$_A$Rs. Nevertheless, selective knockout experiments indicate that these α5-GABA$_A$Rs are not etomidate's essential targets (29). This curious combination of findings suggests that there are subcircuits within the hippocampus that are enriched in α5 subunits at multiple levels. Our present results suggest that these circuits also incorporate β2 subunits, and that they control LTP initiated by theta-burst stimuli in vitro. In vivo, both O-LM and neurogliaform/ivy cells exhibit activity that is time-locked to θ-oscillations (62); θ-oscillations in turn are intimately involved in hippocampal function, including spatial learning and memory (63). Modulation of θ-oscillations by etomidate is altered in β3-GABA$_A$R KO mice (42), but the strength of cross-frequency coupling between θ-γ is unaffected, as is the transient suppression of fast inhibition that has been proposed to play a role in this phenomenon (64). These findings suggest the testable hypothesis that β2-GABA$_A$R modulation of cross-frequency coupling through interneurons may therefore be instrumental in etomidate's effects.

ACKNOWLEDGMENTS

We thank Harald Hentschke (Department of Anesthesiology, University Wisconsin-Madison) for providing custom written routines in MATLAB for analysis of electrophysiological data, and Mark Perkins (Department of Anesthesiology, University of Wisconsin-Madison) for excellent technical support.

Present address of Claudia Benkwitz: Dept. of Anesthesia and Perioperative Care, University of California, San Francisco, California (claudia.benkwitz@ucsf.edu).

GRANTS

This study was supported by National Institutes of Health (NIH) Grants GM118801 (to R.A.P.), AA010422 (to G.E.H.), AA020889 (to

G.E.H.), and the Ralph M. Waters Professorship (to R.A.P.) of the Department of Anesthesiology, University of Wisconsin-Madison.

DISCLOSURES

No conflicts of interest, financial or otherwise, are declared by the authors.

AUTHOR CONTRIBUTIONS

C.B., G.E.H., and R.A.P. conceived and designed research; A.G.F., C.B., G.S., and N.K. performed experiments; A.G.F., C.B., G.S., and R.A.P. analyzed data; G.E.H. and R.A.P. interpreted results of experiments; A.G.F., C.B., and R.A.P. prepared figures; A.G.F., C.B., and R.A.P. drafted manuscript; A.G.F., C.B., G.S., N.K., G.E.H., and R.A.P. approved final version of manuscript.

REFERENCES

1. **Hemmings HC**, **Riegelhaupt PM**, **Kelz MB**, **Solt K**, **Eckenhoff RG**, **Orser BA**, **Goldstein PA.** Towards a comprehensive understanding of anesthetic mechanisms of action: a decade of discovery. *Trends Pharmacol Sci* 40: 464–481, 2019. doi:10.1016/j.tips.2019.05.001.
2. **Garcia PS**, **Kolesky SE**, **Jenkins A.** General anesthetic actions on GABA(A) receptors. *Curr Neuropharmacol* 8: 2–9, 2010. doi:10.2174/157015910790909502.
3. **Franks NP.** General anaesthesia: from molecular targets to neuronal pathways of sleep and arousal. *Nat Rev Neurosci* 9: 370–386, 2008. doi:10.1038/nrn2372.
4. **Antkowiak B**, **Rammes G.** GABA(A) receptor-targeted drug development -new perspectives in perioperative anesthesia. *Expert Opin Drug Discov* 14: 683–699, 2019. doi:10.1080/17460441.2019.1599356.
5. **Weir CJ**, **Mitchell SJ**, **Lambert JJ.** Role of GABA(A) receptor subtypes in the behavioural effects of intravenous general anaesthetics. *Br J Anaesth* 119: I167–I175, 2017. doi:10.1093/bja/aex369.
6. **Macdonald RL**, **Olsen RW.** GABAA receptor channels. *Annu Rev Neurosci* 17: 569–602, 1994. doi:10.1146/annurev.ne.17.030194.003033.
7. **Olsen RW**, **Sieghart W.** International union of pharmacology. LXX. Subtypes of gamma-aminobutyric acid(A) receptors: classification on the basis of subunit composition, pharmacology, and function. Update. *Pharmacol Rev* 60: 243–260, 2008. doi:10.1124/pr.108.00505.
8. **Olsen RW.** GABA(A) receptor: positive and negative allosteric modulators. *Neuropharmacology* 136: 10–22, 2018. doi:10.1016/j.neuropharm.2018.01.036.
9. **Mody I**, **Pearce RA.** Diversity of inhibitory neurotransmission through GABA(A) receptors. *Trends Neurosci* 27: 569–575, 2004. doi:10.1016/j.tins.2004.07.002.
10. **Belelli D**, **Lambert JJ**, **Peters JA**, **Wafford K**, **Whiting PJ.** The interaction of the general anesthetic etomidate with the gamma-aminobutyric acid type A receptor is influenced by a single amino acid. *Proc Natl Acad Sci USA* 94: 11031–11036, 1997. doi:10.1073/pnas.94.20.11031.
11. **Siegwart R**, **Jurd R**, **Rudolph U.** Molecular determinants for the action of general anesthetics at recombinant alpha(2)beta(3)gamma (2) gamma-aminobutyric acid(A) receptors. *J Neurochem* 80: 140–148, 2002. doi:10.1046/j.0022-3042.2001.00682.x.
12. **Lor C**, **Perouansky M**, **Pearce RA.** Isoflurane potentiation of GABAA receptors is reduced but not eliminated by the β3($N_2$65M) mutation. *Int J Mol Sci* 21: 9534, 2020. doi:10.3390/ijms21249534.
13. **Zeller A**, **Arras M**, **Lazaris A**, **Jurd R**, **Rudolph U.** Distinct molecular targets for the central respiratory and cardiac actions of the general anesthetics etomidate and propofol. *FASEB J* 19: 1677–1679, 2005. doi:10.1096/fj.04-3443fje.
14. **Jurd R**, **Arras M**, **Lambert S**, **Drexler B**, **Siegwart R**, **Crestani F**, **Zaugg M**, **Vogt KE**, **Ledermann B**, **Antkowiak B**, **Rudolph U.** General anesthetic actions in vivo strongly attenuated by a point mutation in the GABA(A) receptor beta3 subunit. *FASEB J* 17: 250–252, 2003. doi:10.1096/fj.02-0611fje.
15. **Reynolds DS**, **Rosahl TW**, **Cirone J**, **O'Meara GF**, **Haythornthwaite A**, **Newman RJ**, **Myers J**, **Sur C**, **Howell O**, **Rutter AR**, **Atack J**, **Macaulay AJ**, **Hadingham KL**, **Hutson PH**, **Belelli D**, **Lambert JJ**, **Dawson GR**, **McKernan R**, **Whiting PJ**, **Wafford KA.** Sedation and anesthesia mediated by distinct GABA(A) receptor isoforms. *J Neurosci* 23: 8608–8617, 2003. doi:10.1523/JNEUROSCI.23-24-08608.2003.
16. **Zarnowska ED**, **Rodgers FC**, **Oh I**, **Rau V**, **Lor C**, **Laha KT**, **Jurd R**, **Rudolph U**, **Eger EIN**, **Pearce RA.** Etomidate blocks LTP and impairs learning but does not enhance tonic inhibition in mice carrying the N265M point mutation in the beta3 subunit of the GABA (A) receptor. *Neuropharmacology* 93: 171–178, 2015. doi:10.1016/j.neuropharm.2015.01.011.
17. **Nicoll RA.** A brief history of long-term potentiation. *Neuron* 93: 281–290, 2017. doi:10.1016/j.neuron.2016.12.015.
18. **Sperk G**, **Schwarzer C**, **Tsunashima K**, **Fuchs K**, **Sieghart W.** GABA (A) receptor subunits in the rat hippocampus I: immunocytochemical distribution of 13 subunits. *Neuroscience* 80: 987–1000, 1997. doi:10.1016/s0306-4522(97)00146-2.
19. **Pirker S**, **Schwarzer C**, **Wieselthaler A**, **Sieghart W**, **Sperk G.** GABA (A) receptors: immunocytochemical distribution of 13 subunits in the adult rat brain. *Neuroscience* 101: 815–850, 2000. doi:10.1016/s0306-4522(00)00442-5.
20. **Cheng VY**, **Martin LJ**, **Elliott EM**, **Kim JH**, **Mount HT**, **Taverna FA**, **Roder JC**, **MacDonald JF**, **Bhambri A**, **Collinson N**, **Wafford KA**, **Orser BA.** α5GABAA receptors mediate the amnestic but not sedative-hypnotic effects of the general anesthetic etomidate. *J Neurosci* 26: 3713–3720, 2006. doi:10.1523/JNEUROSCI.5024-05.2006.
21. **Orser BA.** Lifting the fog around anesthesia. *Sci Am* 296: 54–61, 2007. doi:10.1038/scientificamerican0607-54.
22. **Martin LJ**, **Oh GH**, **Orser BA.** Etomidate targets $\alpha^5\gamma$-aminobutyric acid subtype A receptors to regulate synaptic plasticity and memory blockade. *Anesthesiology* 111: 1025–1035, 2009. doi:10.1097/ALN.0b013e3181bbc961.
23. **Ju YH**, **Guzzo A**, **Chiu MW**, **Taylor P**, **Moran MF**, **Gurd JW**, **MacDonald JF**, **Orser BA.** Distinct properties of murine α5 γ-aminobutyric acid type a receptors revealed by biochemical fractionation and mass spectroscopy. *J Neurosci Res* 87: 1737–1747, 2009. doi:10.1002/jnr.21991.
24. **Burgard EC**, **Tietz EI**, **Neelands TR**, **Macdonald RL.** Properties of recombinant γ-aminobutyric acid A receptor isoforms containing the α5subunit subtype. *Mol Pharmacol* 50: 119–127, 1996.
25. **Sur C**, **Quirk K**, **Dewar D**, **Atack J**, **McKernan R.** Rat and human hippocampal α5 subunit-containing γ–aminobutyric Acid$_A$ receptors have α5β3γ2 pharmacological characteristics. *Mol Pharmacol* 54: 928–933, 1998. doi:10.1124/mol.54.5.928.
26. **Schulz JM**, **Knoflach F**, **Hernandez MC**, **Bischofberger J.** Enhanced dendritic inhibition and impaired NMDAR activation in a mouse model of down syndrome. *J Neurosci* 39: 5210–5221, 2019. doi:10.1523/JNEUROSCI.2723-18.2019.
27. **Schulz JM**, **Knoflach F**, **Hernandez MC**, **Bischofberger J.** Dendrite-targeting interneurons control synaptic NMDA-receptor activation via nonlinear α5-GABAA receptors. *Nat Commun* 9: 3576, 2018. doi:10.1038/s41467-018-06004-8.
28. **Isaacson JS**, **Scanziani M.** How inhibition shapes cortical activity. *Neuron* 72: 231–243, 2011. doi:10.1016/j.neuron.2011.09.027.
29. **Rodgers FC**, **Zarnowska ED**, **Laha KT**, **Engin E**, **Zeller A**, **Keist R**, **Rudolph U**, **Pearce RA.** Etomidate impairs long-term potentiation in vitro by targeting α5-subunit containing GABAA receptors on nonpyramidal cells. *J Neurosci* 35: 9707–9716, 2015. doi:10.1523/JNEUROSCI.0315-15.2015.
30. **Harris KD**, **Hochgerner H**, **Skene NG**, **Magno L**, **Katona L**, **Bengtsson Gonzales C**, **Somogyi P**, **Kessaris N**, **Linnarsson S**, **Hjerling-Leffler J.** Classes and continua of hippocampal CA1 inhibitory neurons revealed by single-cell transcriptomics. *PLoS Biol* 16: e2006387, 2018. doi:10.1371/journal.pbio.2006387.
31. **Miralles CP**, **Li M**, **Mehta AK**, **Khan ZU**, **De Blas AL.** Immunocytochemical localization of the β3 subunit of the γ-aminobutyric acid$_A$ receptor in the rat brain. *J Comp Neurol* 413: 535–548, 1999. doi:10.1002/(SICI)1096-9861(19991101)413:4<535::AID-CNE4>3.0.CO;2-T.
32. **Blednov YA**, **Borghese CM**, **Ruiz CI**, **Cullins MA**, **Da Costa A**, **Osterndorff-Kahanek EA**, **Homanics GE**, **Harris RA.** Mutation of the inhibitory ethanol site in GABAA ρ1 receptors promotes tolerance to ethanol-induced motor incoordination. *Neuropharmacology* 123: 201–209, 2017. doi:10.1016/j.neuropharm.2017.06.013.

33. **Pearce RA.** Physiological evidence for two distinct GABAA responses in rat hippocampus. *Neuron* 10: 189–200, 1993. doi:10.1016/0896-6273(93)90310-n.
34. **Benkwitz C**, **Liao M**, **Laster MJ**, **Sonner JM**, **Eger EI 2nd**, **Pearce RA.** Determination of the EC50 amnesic concentration of etomidate and its diffusion profile in brain tissue: implications for in vitro studies. *Anesthesiology* 106: 114–123, 2007. doi:10.1097/00000542-200701000-00020.
35. **Maccaferri G**, **Roberts JDB**, **Szucs P**, **Cottingham CA**, **Somogyi P.** Cell surface domain specific postsynaptic currents evoked by identified GABAergic neurones in rat hippocampus in vitro. *J Physiol* 524: 91–116, 2000 [Erratum in *J Physiol* 528: 669, 2000]. doi:10.1111/j.1469-7793.2000.t01-3-00091.x.
36. **Pouille F**, **Scanziani M.** Routing of spike series by dynamic circuits in the hippocampus. *Nature* 429: 717–723, 2004. doi:10.1038/nature02615.
37. **Amadeu ME**, **Abramowicz AE**, **Chambers G**, **Cottrell JE**, **Kass IS.** Etomidate does not alter recovery after anoxia of evoked population spikes recorded from the CA1 region of rat hippocampal slices. *Anesthesiology* 88: 1274–1280, 1998. doi:10.1097/00000542-199805000-00019.
38. **Grover LM**, **Kim E**, **Cooke JD**, **Holmes WR.** LTP in hippocampal area CA1 is induced by burst stimulation over a broad frequency range centered around delta. *Learn Mem* 16: 69–81, 2009. doi:10.1101/lm.1179109.
39. **Ali AB**, **Thomson AM.** Synaptic α5 subunit-containing GABAA receptors mediate IPSPs elicited by dendrite-preferring cells in rat neocortex. *Cereb Cortex* 18: 1260–1271, 2008. doi:10.1093/cercor/bhm160.
40. **Zarnowska ED**, **Keist R**, **Rudolph U**, **Pearce RA.** GABAA Receptor α5 subunits contribute to GABA$_{A,slow}$ synaptic inhibition in mouse hippocampus. *J Neurophysiol* 101: 1179–1191, 2009. doi:10.1152/jn.91203.2008.
41. **Caraiscos VB**, **Elliott EM**, **You T**, **Cheng VY**, **Belelli D**, **Newell JG**, **Jackson MF**, **Lambert JJ**, **Rosahl TW**, **Wafford KA**, **MacDonald JF**, **Orser BA.** Tonic inhibition in mouse hippocampal CA1 pyramidal neurons is mediated by α5 subunit-containing γ-aminobutyric acid type A receptors. *Proc Natl Acad Sci USA* 101: 3662–3667, 2004. doi:10.1073/pnas.0307231101.
42. **Hentschke H**, **Benkwitz C**, **Banks MI**, **Perkins MG**, **Homanics GE**, **Pearce RA.** Altered GABA$_{A,slow}$ inhibition and network oscillations in mice lacking the GABA$_A$ receptor β3 subunit. *J Neurophysiol* 102: 3643–3655, 2009. doi:10.1152/jn.00651.2009.
43. **Prenosil GA**, **Schneider Gasser EM**, **Rudolph U**, **Keist R**, **Fritschy JM**, **Vogt KE.** Specific subtypes of GABAA receptors mediate phasic and tonic forms of inhibition in hippocampal pyramidal neurons. *J Neurophysiol* 96: 846–857, 2006. doi:10.1152/jn.01199.2005.
44. **Hausrat TJ**, **Muhia M**, **Gerrow K**, **Thomas P**, **Hirdes W**, **Tsukita S**, **Heisler FF**, **Herich L**, **Dubroqua S**, **Breiden P**, **Feldon J**, **Schwarz JR**, **Yee BK**, **Smart TG**, **Triller A**, **Kneussel M.** Radixin regulates synaptic GABAA receptor density and is essential for reversal learning and short-term memory. *Nat Commun* 6: 6872, 2015. doi:10.1038/ncomms7872.
45. **Gasparini S**, **Migliore M**, **Magee JC.** On the initiation and propagation of dendritic spikes in CA1 pyramidal neurons. *J Neurosci* 24: 11046–11056, 2004. doi:10.1523/JNEUROSCI.2520-04.2004.
46. **Elfant D**, **Pál BZ**, **Emptage N**, **Capogna M.** Specific inhibitory synapses shift the balance from feedforward to feedback inhibition of hippocampal CA1 pyramidal cells. *Eur J Neurosci* 27: 104–113, 2008. doi:10.1111/j.1460-9568.2007.06001.x.
47. **Milstein AD**, **Bloss EB**, **Apostolides PF**, **Vaidya SP**, **Dilly GA**, **Zemelman BV**, **Magee JC.** Inhibitory gating of input comparison in the CA1 microcircuit. *Neuron* 87: 1274–1289, 2015. doi:10.1016/j.neuron.2015.08.025.
48. **Olsen RW**, **Sieghart W.** GABA$_A$ receptors: subtypes provide diversity of function and pharmacology. *Neuropharmacology* 56: 141–148, 2009. doi:10.1016/j.neuropharm.2008.07.045.
49. **Chen X**, **Keramidas A**, **Lynch JW.** Physiological and pharmacological properties of inhibitory postsynaptic currents mediated by alpha5beta1gamma2, α5β2γ2 and α5β3γ2 GABAA receptors. *Neuropharmacology* 125: 243–253, 2017. doi:10.1016/j.neuropharm.2017.07.027.
50. **Karayannis T**, **Elfant D**, **Huerta-Ocampo I**, **Teki S**, **Scott RS**, **Rusakov DA**, **Jones MV**, **Capogna M.** Slow GABA transient and receptor desensitization shape synaptic responses evoked by hippocampal neurogliaform cells. *J Neurosci* 30: 9898–9909, 2010. doi:10.1523/JNEUROSCI.5883-09.2010.
51. **Armstrong C**, **Krook-Magnuson E**, **Soltesz I.** Neurogliaform and ivy cells: a major family of nNOS expressing GABAergic neurons. *Front Neural Circuits* 6: 23, 2012. doi:10.3389/fncir.2012.00023.
52. **Krook-Magnuson E**, **Luu L**, **Lee SH**, **Varga C**, **Soltesz I.** Ivy and neurogliaform interneurons are a major target of μ-opioid receptor modulation. *J Neurosci* 31: 14861–14870, 2011. doi:10.1523/JNEUROSCI.2269-11.2011.
53. **Markwardt SJ**, **Dieni CV**, **Wadiche JI**, **Overstreet-Wadiche L.** Ivy/neurogliaform interneurons coordinate activity in the neurogenic niche. *Nat Neurosci* 14: 1407–1409, 2011. doi:10.1038/nn.2935.
54. **Fuentealba P**, **Begum R**, **Capogna M**, **Jinno S**, **Marton LF**, **Csicsvari J**, **Thomson A**, **Somogyi P**, **Klausberger T.** Ivy cells: a population of nitric-oxide-producing, slow-spiking GABAergic neurons and their involvement in hippocampal network activity. *Neuron* 57: 917–929, 2008 [Erratum in *Neuron* 58: 295, 2008]. doi:10.1016/j.neuron.2008.01.034.
55. **Capogna M.** Neurogliaform cells and other interneurons of stratum lacunosum-moleculare gate entorhinal-hippocampal dialogue. *J Physiol* 589: 1875–1883, 2011. doi:10.1113/jphysiol.2010.201004.
56. **Price CJ**, **Cauli B**, **Kovacs ER**, **Kulik A**, **Lambolez B**, **Shigemoto R**, **Capogna M.** Neurogliaform neurons form a novel inhibitory network in the hippocampal CA1 area. *J Neurosci* 25: 6775–6786, 2005. doi:10.1523/JNEUROSCI.1135-05.2005.
57. **Cembrowski MS**, **Bachman JL**, **Wang L**, **Sugino K**, **Shields BC**, **Spruston N.** Spatial gene-expression gradients underlie prominent heterogeneity of CA1 pyramidal neurons. *Neuron* 89: 351–368, 2016. doi:10.1016/j.neuron.2015.12.013.
58. **Salesse C**, **Mueller CL**, **Chamberland S**, **Topolnik L.** Age-dependent remodelling of inhibitory synapses onto hippocampal CA$_1$ oriens-lacunosum moleculare interneurons. *J Physiol* 589: 4885–4901, 2011. doi:10.1113/jphysiol.2011.215244.
59. **Cembrowski MS**, **Wang L**, **Sugino K**, **Shields BC**, **Spruston N.** Hipposeq: a comprehensive RNA-seq database of gene expression in hippocampal principal neurons. *eLife* 5: e14997, 2016. doi:10.7554/eLife.14997.
60. **Magnin E**, **Francavilla R**, **Amalyan S**, **Gervais E**, **David LS**, **Luo X**, **Topolnik L.** Input-specific synaptic location and function of the α5 GABAA receptor subunit in the mouse CA1 hippocampal neurons. *J Neurosci* 39: 788–801, 2019. doi:10.1523/JNEUROSCI.0567-18.2018.
61. **Leão RN**, **Mikulovic S**, **Leão KE**, **Munguba H**, **Gezelius H**, **Enjin A**, **Patra K**, **Eriksson A**, **Loew LM**, **Tort AB**, **Kullander K.** OLM interneurons differentially modulate CA3 and entorhinal inputs to hippocampal CA1 neurons. *Nat Neurosci* 15: 1524–1530, 2012. doi:10.1038/nn.3235.
62. **Klausberger T**, **Somogyi P.** Neuronal diversity and temporal dynamics: the unity of hippocampal circuit operations. *Science* 321: 53–57, 2008. doi:10.1126/science.1149381.
63. **Buzsáki G**, **Moser EI.** Memory, navigation and theta rhythm in the hippocampal-entorhinal system. *Nat Neurosci* 16: 130–138, 2013. doi:10.1038/nn.3304.
64. **White JA**, **Banks MI**, **Pearce RA**, **Kopell NJ.** Networks of interneurons with fast and slow gamma-aminobutyric acid type A (GABAA) kinetics provide substrate for mixed gamma-theta rhythm. *Proc Natl Acad Sci USA* 97: 8128–8133, 2000. doi:10.1073/pnas.100124097.